ACS Medicinal Chemistry Letters

pubs.acs.org/acsmedchemlett Letter

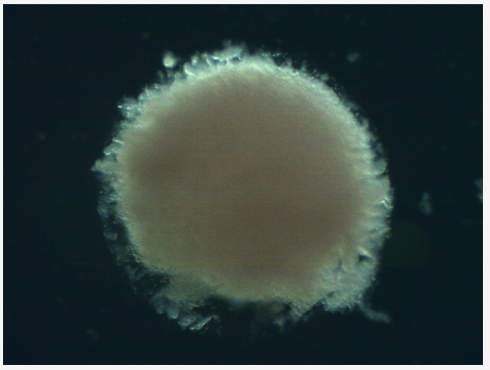
Characterization of an Alginate Encapsulated LS180 Spheroid Model for Anti-colorectal Cancer Compound Screening

Tanya Smit, Carlemi Calitz, Clarissa Willers, Hanna Svitina, Josias Hamman, Stephen J. Fey, Chrisna Gouws,* and Krzysztof Wrzesinski*

Cite This: https://dx.doi.org/10.1021/acsmedchemlett.0c00076 Read Online

ACCESS | Metrics & More | Article Recommendations | Supporting Information

ABSTRACT: Colorectal cancer is one of the leading causes of cancer-related deaths. A main problem for its treatment is resistance to chemotherapy, requiring the development of new drugs. The success rate of new candidate cancer drugs in clinical trials remains dismal. Three-dimensional (3D) cell culture models have been proposed to bridge the current gap between *in vitro* chemotherapeutic studies and the human *in vivo*, due to shortcomings in the physiological relevance of the commonly used two-dimensional cell culture models. In this study, LS180 colorectal cancer cells were cultured as 3D sodium alginate encapsulated spheroids in clinostat bioreactors. Growth and viability were evaluated for 20 days to determine the ideal experimental window. The 3- (4,5- dimethylthiazol- 2- yl)-2,5- diphenyltetrazolium bromide assay was then used to establish half maximal inhibitory concentrations for the standard chemotherapeutic drug, paclitaxel. This concentration was used to further evaluate the established 3D model. During model characterization and evaluation soluble protein content, intracellular adenosine triphosphate levels, extracellular adenylate kinase, glucose consumption, and P-glycoprotein (P-gp) gene expression were measured. Use of the model for chemotherapeutic treatment screening was evaluated using two concentrations of paclitaxel, and treatment continued for 96 h. Paclitaxel caused a decrease in cell growth, viability, and glucose consumption in the model. Furthermore, relative expression of P-gp increased compared to the untreated control group. This is a typical resistance-producing change, seen *in vivo* and known to be a result of paclitaxel treatment. It was concluded that the LS180 sodium alginate encapsulated spheroid model could be used for testing new chemotherapeutic compounds for colorectal cancer.



KEYWORDS: *Colorectal cancer, LS180, clinostat bioreactors, spheroids, sodium alginate, three-dimensional cell culture*

Downloaded via BIU SANTE on April 20, 2020 at 10:23:16 (UTC).
See https://pubs.acs.org/sharingguidelines for options on how to legitimately share published articles.

Cancer remains a global burden, and finding new chemotherapeutic drugs is still crucial in drug discovery and development. Colorectal cancer is the most common type of gastrointestinal malignancy, with nearly 145,000 new cases reported annually in the USA,[1] and is often detected only in its advanced stages.[2] The main problems for treatment are chemotherapy resistance development and progression to metastatic cancer.[3]

Several treatment options are available including surgery, chemotherapy, radiation therapy, immunotherapy, and nutritional support therapy.[2] The treatment method selected is dependent on the location and the stage of the tumor.[4,5] However, the backbone of first-line treatment chemotherapy is a fluoropyrimidine (like fluorouracil) in various combinations and schedules.[6] Paclitaxel is widely used for various cancer types and has been shown to be active against colorectal cancer cells and acts by stabilizing microtubules, leading to apoptosis.[7]

Currently, the preclinical identification of new chemotherapeutic agents relies on *in vitro* cell line models and *in vivo* animal models. The use of animals in research is a sensitive ethical topic, with the United States Environmental Protection Agency announcing a 2035 deadline for their elimination from research.[8] Implementation of the 3 "R's" (Reduction, Replacement, and Refinement) through *in silico* or *in vitro* assays has become an essential element of risk management in nonclinical and preclinical stages,[9] requiring new and improved high throughput *in vitro* models and assays.[10,11] Thus, *in vitro* studies aimed at understanding the molecular progression of cancer or identifying effective chemotherapeutic agents (whether derived from natural products or synthesized *de novo*) rely on a pathophysiological model which closely mimics the tumor and microenvironment *in vivo*.[12]

Tumor-derived cell lines are often used as *in vitro* models despite the fact that they carry millions of deviations from the tumors from which they originated and often lack physiological

Special Issue: In Memory of Maurizio Botta: His Vision of Medicinal Chemistry

Received: February 12, 2020
Accepted: March 31, 2020

© XXXX American Chemical Society

relevance.[13,14] This contributes to the problem of only about 3.4% of cancer drug candidates being successful in clinical trials.[15] New models with better correlation are therefore urgently needed.

Human colorectal cancer cell lines are commonly used in preclinical systems and have provided many insights into tumor and cell biology.[16] One example, the microvillus expressing LS180 cell line, has been extensively characterized and used for various *in vitro* studies including chemotherapeutic screening.[17] It has been reported to express many CYP450 isoforms, including CYP1A2 and CYP3A4[18−20] and is an excellent cell line to study CYP450 induction, especially as it expresses the pregnane X receptor (PXR).[21]

Since the early 1950s cells, cultured either in suspension or on flat surfaces as two-dimensional (2D) monolayers, have contributed to the establishment of a myriad of drug candidates. Although convenient, these systems have disadvantages due to deficient cellular communication as compared to cells *in vivo* and their short growth time period.[22,23] Novel three-dimensional (3D) cell culturing techniques attempt to overcome these obstacles by providing a cellular environment more closely related to the *in vivo* state, increasing the predictability of drug efficacy and toxicity prior to the initiation of clinical trials.[22−25]

Spheroids are simple 3D models that most effectively recapitulate not only structural but also physiological and biological features of tumors *in vitro*.[26] Spheroids can be created from a wide variety of cell types due to the tendency of adherent cells to aggregate.[27] In this study, LS180 cells were cultured as cell spheroids. There are several approaches to maintain, expand, and differentiate these spheroid cultures, using different 3D culture systems.[28] One such a system is the dynamic clinostat-based rotating bioreactor and BioArray Matrix drive (BAM) system.[24] Bioreactors are devices in which spheroids develop under closely monitored and tightly controlled environmental operating conditions (i.e., pH, temperature, shear stress, pressure, nutrient supply, and waste removal).[29] Bioreactors induce the mixing of oxygen and nutrients throughout the medium, reducing the concentration boundary layer commonly found in static cultures.[30]

Various methods can be employed to construct 3D spheroids, one of which entails encapsulating a single cell suspension in substances with gelling properties.[31] Alginates are anionic polysaccharides extracted from brown seaweed, composed of β-D-mannuronic acid and α-L-guluronic acid. These alginates form hydrogels when cross-linked with multivalent cations, such as Ca^{2+}, Ba^{2+}, or Fe^{2+}.[32] Alginates cross-linked with Ca^{2+} have been popularized for *in vitro* cell culture and tissue engineering applications due to their biocompatibility, low toxicity, relatively low cost, and mild gelation properties.[33,34] They have a relatively inert aqueous environment and high gel porosity (which allows for high diffusion rates) and are biodegradable.[35−37]

Purified alginate gels have been shown to support proliferation of rat marrow cells and their differentiation along the osteoblastic lineage after encapsulation. This indicates that sodium alginate has potential to act as a tissue-engineering scaffold on which tissues may be formed.[38] Alginate gels are especially useful when creating spheroids of cell lines which do not naturally aggregate or aggregate poorly, like the LS180 cell line.

Establishing new 3D cell culturing systems to evaluate anticancer potential of drugs will be a valuable asset for future research, having the potential to bridge the gap between *in vitro* research and the *in vivo* situation without using animal models. The aim of this study was, therefore, to create a new 3D colorectal cancer cell culture model based on LS180 cells, by combining the dynamic clinostat bioreactor technique with the microencapsulation technique using sodium alginate. This model was then characterized before validating its use as a cancer treatment screening tool by evaluating its reactivity to treatment with the standard chemotherapeutic drug, paclitaxel.

The following parameters were measured as an indication of cell viability: intracellular adenosine triphosphate (ATP) content, extracellular adenylate kinase (AK) release, and glucose consumption. Cell growth, in terms of soluble protein content, was also measured. Relative expression of the P-glycoprotein (P-gp) gene was measured using a real-time reverse transcription polymerase chain reaction-based (qRT-PCR) assay.

TWO-DIMENSIONAL ANTICANCER ACTIVITY PRESCREENING

The anticancer activity of paclitaxel was first evaluated in 2D cultures of the LS180 cell line, employing the 3-(4,5-dimethylthiazol-2-yl)-2,5-diphenyl tetrazolium bromide (MTT) assay. This was done to estimate the 50% inhibitory concentration (IC_{50}) per protein content relative to an untreated control. LS180 cells were treated with increasing paclitaxel concentrations for 96 h, and the cell viability was determined with the MTT assay. The data was analyzed with the Probit regression analysis tool to calculate the IC_{50} concentrations (binominal response variable).[39] In this study, the data was used to determine paclitaxel's IC_{50} value at 95% confidence limits.

The IC_{50} of paclitaxel, relative to an untreated control, in 2D LS180 cells treated for 96 h was 94.6 nM (81.5 nM to 108.9 nM 95% confidence limits). Reduced LS180 cell viability was observed at concentrations above 9.0 nM paclitaxel. The IC_{75} value in 2D LS180 cells was calculated to be 613.8 nM for paclitaxel. Treatment with 1 μM paclitaxel resulted in a lower percentage of cell viability inhibition (73.9%). This was indicative of drug resistance that started to occur against paclitaxel in this cell line at the highest concentration applied.

The IC_{50} concentration determined here fell within the known active ranges for the drug. Rossouw studied the effects of paclitaxel on various cell lines, including a noncancerous porcine kidney cell line (LLC-PK1).[40] The IC_{50} concentration observed following 96 h exposure in this cell line was 29.7 nM. In the small cell lung cancer (SCLC) cell line (HCI-H69 V), the IC_{50} concentration was found to be 2.8 nM. Lastly, paclitaxel was tested on drug resistant SCLC cell lines (H69AR and NCI-H69/LX4), with their IC_{50} concentrations estimated at 4.8 nM and 613.1 nM, respectively. This showed the high level of variability in *in vitro* activity between different cancer types. Rossouw[40] also indicated that SCLC cells underwent adaptations as a coping mechanism after exposure to paclitaxel. These cell models can eventually reach a threshold of cytotoxicity, and then multidrug resistance will emerge. This correlates with our findings where the relative percentage cell viability inhibition decreased as the dose reached 1.0 mM (results not shown).

https://dx.doi.org/10.1021/acsmedchemlett.0c00076
ACS Med. Chem. Lett. XXXX, XXX, XXX−XXX

PREPARATION OF SODIUM ALGINATE ENCAPSULATED LS180 CELL SPHEROIDS

The sodium alginate encapsulation of LS180 cells was optimized and applied in this study. Parameters investigated during the optimization of the method included sodium alginate concentrations, spheroid volume, cell concentration, cross-linker volume, and incubation time, as well as finding a quick and practical way to form the spheroids.

The optimized method had 2,000 cells cultured as 3D encapsulated spheroids using 2.5% w/v sodium alginate, in 1 μL droplets (Figure 1a). After adding the cross-linker solution and incubating for 5 min, the hemispherical spheroids were collected into growth medium and transferred to clinostat bioreactors (Figure 1b). Rotation speed of the drive unit was adjusted to ensure that spheroids remained in an essentially stationary position relative to the bioreactor throughout the experiment. Photographs of sodium alginate encapsulated LS180 cell spheroids at different stages are shown in Figure 1.

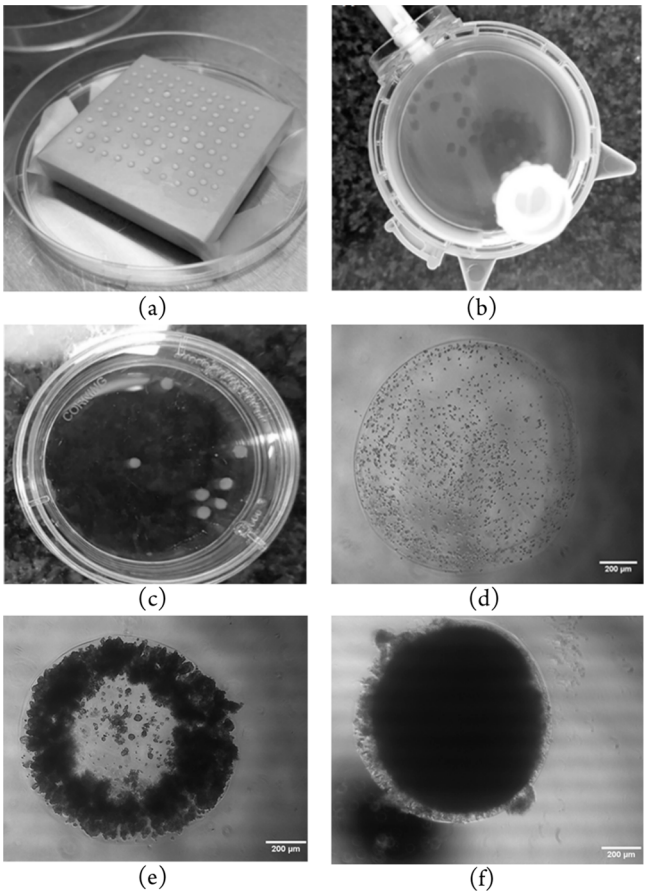


Figure 1. Photographs of LS180 cells encapsulated in 2.5% *w/v* sodium alginate solution at different stages: (a) Drops of cell suspension in sodium alginate solution on a square block, treated with cross-linker solution prior to transfer to bioreactors; (b) 21 day old encapsulated LS180 cell spheroids in a rotating bioreactor; (c) 21 day old encapsulated LS180 cell spheroids, photographed in a Petri dish; (d) LS180 cells in a spheroid directly after sodium alginate encapsulation before transfer to a bioreactor; (e) encapsulated LS180 spheroid 8 days after transfer to a bioreactor; (f) encapsulated LS180 spheroid 20 days after transfer to a bioreactor.

CHARACTERIZATION OF THE LS180 SODIUM ALGINATE ENCAPSULATED SPHEROID MODEL

During the development and maintenance of multicellular organisms, there must be a balance between cell division and cell death.[41] According to Ahmann et al.,[42] ATP levels are linearly related to the number of viable cells and that will increase with time, correlating to growth kinetics. The ATP content of 3D cell cultures is therefore a powerful tool to predict health, growth, and energy status with high confidence.[43] When cells die, ATP levels may fall rapidly due to ATPases.[42] In order for cells to undergo apoptosis, adequate amounts of intracellular ATP levels are required. If ATP depletion has occurred, cells will still die, but their demise will be necrotic.[44]

Cell death is an important variable in cancer development.[45] Apoptosis occurs normally during development and aging of normal tissues and serves as a homeostatic mechanism to maintain cell populations in tissues.[46] Another parameter that can measure cell death is AK since it is an intramitochondrial enzyme that is released into the extracellular space upon cell lysis.[47] When mammalian cells interact with toxins, they undergo a series of dramatic structural and morphological changes, which can lead to loss of membrane integrity.[48] Cytotoxicity can therefore be detected by the presence of extracellular AK, and this serves as an important marker of cell death.[49]

The LS180 sodium alginate encapsulated spheroid model was cultured, maintained, and characterized for 20 days. This was important as it has previously been shown that cancer cells typically need at least 18 days to reach an equilibrium in 3D cultures.[25,50] To evaluate the viability and growth, intracellular ATP and extracellular AK levels were measured, and the data was normalized per microgram of soluble protein to correct for changes in cell numbers (Figure 2).

There was a consistent slow increase in soluble protein content in the LS180 cell spheroids until day 10 followed by a substantial increase. All bioreactors contained 300 LS180 cell spheroids from day 0−10. The number of spheroids was then reduced to 150 spheroids per bioreactor by splitting following sampling on day 10. This resulted in a greater abundance of nutrients per cell. This may have caused the sudden increase in soluble protein content. The slower growth from day 0 to 10 could have been a result of recovery from trypsinization during which spheroids are engaged in restoring key functions.[50] Clearly, this was not the only contributing factor to the protein content increase (because halving of the number of spheroids led to a 5-fold increase in the amount of protein per spheroid). Other factors that should be considered include the growth phase of the cells, the time elapsed since trypsinisation, and acclimatization to the 3D environment. The cellular protein content increase, from day 13−20, was statistically significantly higher ($p < 0.001$) than the initial protein content at time 0. Photographs reveal that there was a substantial difference in the number of cells per spheroid over time (Figure 1d−f). On day 15 the population was further reduced to 50 spheroids per bioreactor.

A steady increase in the intracellular ATP content per μg protein could be observed during the first 10 days (Figure 2b). The decrease of intracellular ATP content per μg protein from day 10 to day 13 corresponded with handling of spheroids (where some spheroids were transferred to another bioreactor). After this, the spheroids started to recover and an

https://dx.doi.org/10.1021/acsmedchemlett.0c00076
ACS Med. Chem. Lett. XXXX, XXX, XXX−XXX

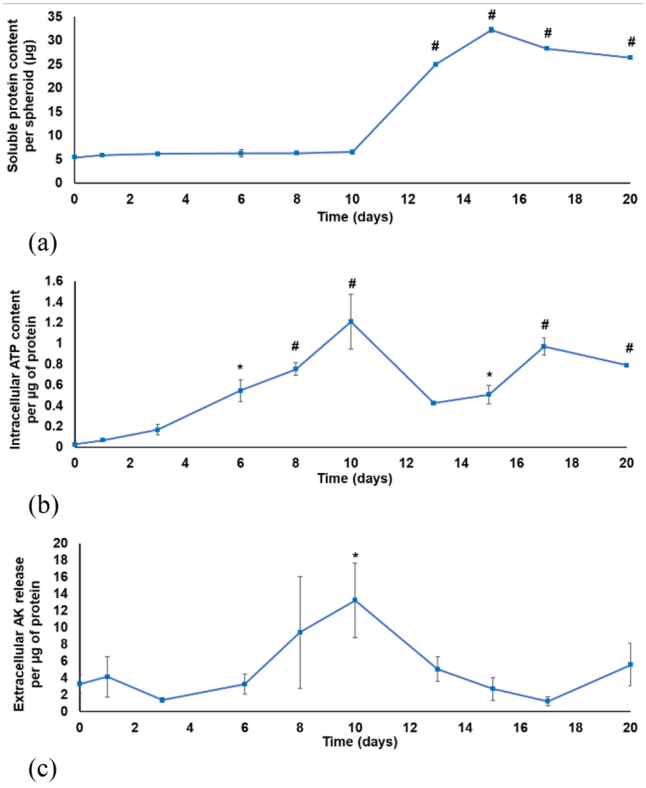


Figure 2. Characterization of the sodium alginate encapsulated LS180 spheroid model as a function of time: (a) Soluble protein content per spheroid (μg protein); (b) intracellular adenosine triphosphate content per μg protein (μM/μg); (c) extracellular adenylate kinase release per μg protein (n = 3, error bars = standard deviation; statistically significant: * = $p < 0.05$; # = $p < 0.001$ (one-way ANOVA followed by the Dunnett posthoc test for comparison with time point 0)).

increase in ATP content was visible, with ATP levels at days 17 and 20 being significantly increased compared to the initial ATP content on day 0 ($p < 0.001$).

The extracellular AK release per μg protein remained relatively low for the first 6 days of culturing (Figure 2c), with a subsequent steady increase until day 10 (relative to day 0, $p < 0.05$) indicating cell death due to competition for nutrient resources. The reduction in the number of spheroids per bioreactor on day 10 resulted in a decrease in the extracellular AK release per μg protein from day 10−17, followed by a slight increase on day 20.

Glucose disappearance from the culture medium indicated metabolic activity during spheroid growth. Fresh medium contains 6.8 mmol/L glucose and was provided each 48 h. After day one, the average glucose content in the spent medium decreased to 3.9 mmol/L, and after 3 days it was below 1.1 mmol/L. From day 6 to 10, the glucose content was below detection limits. Even following the reduction in spheroid density on days 10 and 15 (where splitting occurred), the glucose was still depleted in the spent culture medium. This indicated that all the glucose in the culture medium was consumed by the LS180 spheroids between the medium changes and that cells in the spheroids were metabolically active. According to Wrzesinski and Fey,[51] the lack of glucose appeared to play a minimal role in the metabolic reprogramming of cells as it causes little stress after prolonged starvation. The small effects that were present appeared to stabilize cellular metabolism and were anti-apoptotic.

Characterization of the model illustrates that there was a steady increase in the intracellular ATP per protein content. The extracellular AK release per protein content also slowly increased as the spheroids aged, possibly indicating apoptosis. However, the intracellular ATP per protein content indicated that cells inside the spheroids were viable despite that AK release also increased. This was supported by the increase and extent of glucose consumption observed over time. The interplay between these parameters indicated that spheroids were actively growing and dying during the characterization period, showing that the sodium alginate encapsulated spheroids were viable for at least 20 days of culturing. C3A cells, in their adaptation to 3D spheroid culture, show similar changes in ATP levels, proliferation rate, and adenylate kinase release.[52]

The spent medium glucose content remained low throughout the characterization period, indicating rapid glucose consumption. It is possible that the low glucose levels could have detrimentally affected spheroid growth. This should be closely monitored.

This characterization allowed an optimal experimental window to be identified for further experiments. The first 10 days were automatically ruled out because of the slow increase in soluble protein content and the expected recovery from trypsinisation. After day 17, there was a slight decrease in the intracellular ATP content per μg protein, with a corresponding increase in the extracellular AK release per μg protein. Although these findings could be attributed to the depletion of nutrients, it was decided not to use the model after day 17 for this study. The experimental window was therefore identified as days 12 to 17.

EVALUATION OF THE LS180 SODIUM ALGINATE ENCAPSULATED SPHEROID MODEL FOR ANTICANCER TREATMENT SCREENING

The standard chemotherapeutic drug, paclitaxel, was employed to evaluate the model's potential for screening of prospective compounds for cancer treatment. Two concentrations of paclitaxel were used, and spheroids were treated every 24 h for 96 h. The doses were determined by dividing the 2D IC_{50} concentration by the soluble protein content per well. This converts the IC_{50} (nM) to LD_{50} (mg compound/mg cellular protein) for easier comparison to *in vivo* blood plasma levels.[24] For the model to be useful to identify potential chemotherapeutic compounds, it is expected that standard chemotherapeutic drugs used to treat colon cancer will have a negative effect on cell viability. Because paclitaxel can activate the xenobiotic receptor[52] treatment would be expected to increase P-gp gene expression.

The soluble protein content per spheroid was measured (using the Bradford assay) during a 96 h exposure to paclitaxel [IC_{50}] and two times the paclitaxel IC_{50} concentration (2[IC_{50}]). All data was normalized to the untreated control group (Figure 3a). It was evident that the soluble protein content per spheroid of the paclitaxel treated groups was similar to that of the untreated spheroids (Figure 3a). It was also notable that there was not a statistically significant difference between the paclitaxel [IC_{50}] treatment group, the paclitaxel 2[IC_{50}], and untreated control. After some initial variation, there was a steady reduction in the intracellular ATP levels per mg protein starting after 24 h for both the paclitaxel

https://dx.doi.org/10.1021/acsmedchemlett.0c00076
ACS Med. Chem. Lett. XXXX, XXX, XXX−XXX

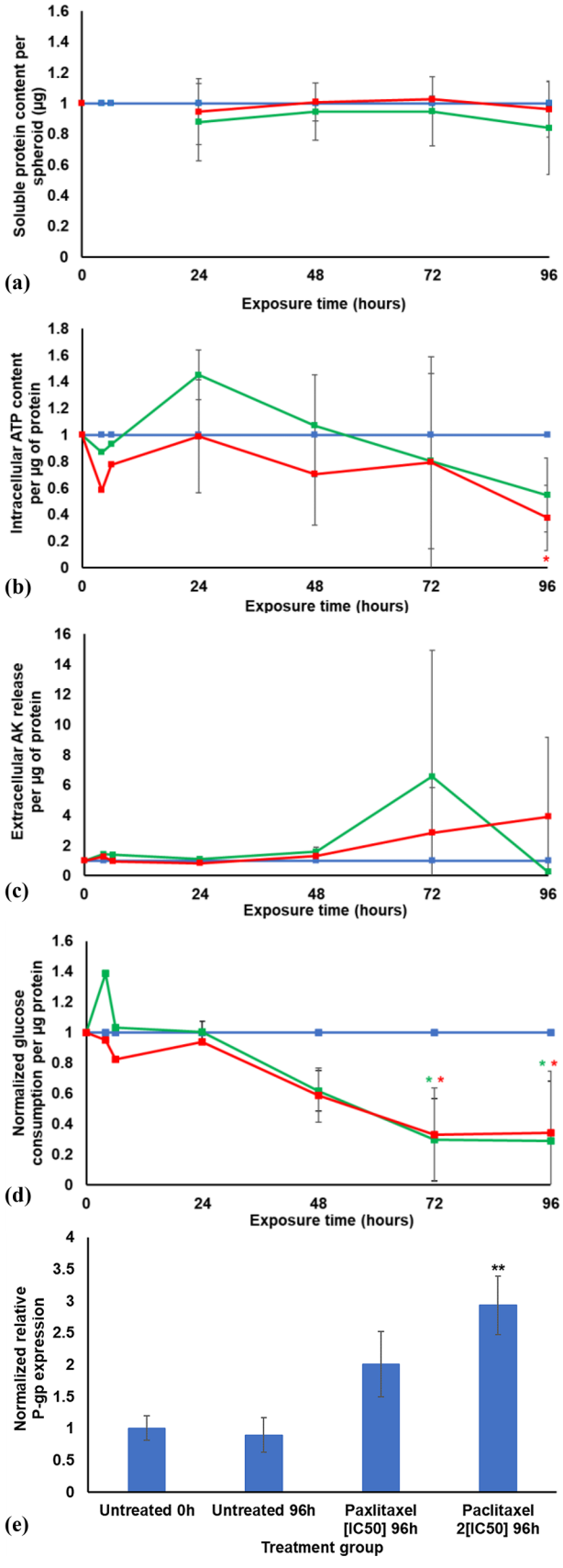


Figure 3. Graphs illustrating the results of the sodium alginate encapsulated LS180 spheroid model during 96 h treatment with paclitaxel, where blue indicates the untreated control group, green indicates the paclitaxel [IC_{50}] treatment group, and red indicates the paclitaxel 2[IC_{50}] treatment group: (a) Normalized soluble protein content (µg) per spheroid; (b) normalized intracellular adenosine triphosphate content per soluble protein (µM/µg); (c) normalized extracellular adenylate kinase release per µg protein; (d) normalized glucose consumption per µg protein. All data was normalized to the untreated control group (n = 2, error bars = standard deviation; * = statistically significant, $p < 0.05$; # = statistically significant, $p < 0.001$ (one-way ANOVA followed by the Dunnett posthoc test for comparison with the untreated control)). (e) Relative P-gp gene expression. All data was normalized to the untreated control group at time point 0 h (n = 3; error bars = standard deviation; ** = statistically significant, $p < 0.01$ (one-way ANOVA followed by the Bonferroni posthoc test for comparison with the untreated control)).

treatment groups relative to the untreated control (Figure 3b). After 96 h exposure, the ATP levels for both treatment groups were reduced to almost half of the untreated group's, with paclitaxel 2[IC_{50}] being statistically significantly decreased relative to the untreated control ($p < 0.05$). This indicated that the treatment with paclitaxel affected the health, growth, and energy status of the LS180 spheroids.

The AK released for both paclitaxel treated groups was not substantially different from the untreated group for the first 48 h of exposure (see Figure 3c). The paclitaxel [IC_{50}] treatment group had a sharp increase in AK release per µg protein at the 72 h time point, followed by a decrease to below the untreated control at 96 h (dead cells cannot release AK). It was notable that the AK release per µg protein following exposure to the higher concentration paclitaxel (2[IC_{50}]) did not reach the high levels seen for the lower paclitaxel concentration ([IC_{50}]). The paclitaxel 2[IC_{50}] concentration had a steady increase in the AK release after 48 h exposure. This suggests that cell death took place at a slower pace in the higher paclitaxel concentration group than in the lower paclitaxel concentration group.

The approximate quantities of glucose consumed by cells in each treatment group (mmol/L) were estimated from the glucose disappearance from the culture medium and corrected for the amount of protein present in the cells. The data were normalized to the glucose consumption per µg protein of the untreated control group (Figure 3d).

Following 6 h exposure to paclitaxel [IC_{50}], there was a marked increase in glucose consumption compared to the untreated control group. Thereafter, there was a strong and steady decline, with very little glucose consumed after 72 h. The paclitaxel 2[IC_{50}] treatment group showed glucose consumption comparable to the control group for the first 24 h followed by a decrease similar to that of the lower dose group (echoing the fall in ATP levels).

Paclitaxel is known to be exported from the cells via P-gp, a broad-specificity efflux pump protein encoded by the gene MDR1 (which plays a pivotal role in the development of drug resistance). The relative expression of the efflux protein, P-gp, was therefore measured before and after exposure (96 h) by means of qRT-PCR.

Treatment with paclitaxel resulted in an increase in P-gp efflux pump gene expression (Figure 3e). Synold et al. demonstrated that paclitaxel induced its own efflux from 2D cultured LS180 cells.[53]

The data presented here indicate that this increase in P-gp expression was dose dependent, and the higher dose showed a statistically significant increase ($p < 0.01$). Li and colleagues[54]

https://dx.doi.org/10.1021/acsmedchemlett.0c00076
ACS Med. Chem. Lett. XXXX, XXX, XXX−XXX

confirmed paclitaxel induced up-regulation of P-gp and that P-gp gene expression can be stimulated by various xenobiotics and clinically administered P-gp substrates.[53]

CONCLUSIONS

3D models have been shown by various sources to be better than their 2D counterparts, as they more closely resemble the *in vivo* situation.[31,55,56] Taken together, the results indicated that the *in vitro* LS180 sodium alginate encapsulated spheroid model can be used for future screening for efficacy of chemotherapeutic compounds (natural or synthesized). The model was viable for up to at least 20 days and revealed the development of resistance to the treatment (via up-regulation of an efflux transporter) in the same way previously observed in patients.

This LS180 sodium alginate encapsulated spheroid model can serve as a new platform for screening of compounds (derived from natural sources or from chemical synthesis) for the treatment of colorectal cancer.

EXPERIMENTAL PROCEDURES

A detailed description of the experimental procedures can be found in the Supporting Information.

ASSOCIATED CONTENT

Supporting Information

The Supporting Information is available free of charge at https://pubs.acs.org/doi/10.1021/acsmedchemlett.0c00076.

Experimental procedures (PDF)

AUTHOR INFORMATION

Corresponding Authors

Chrisna Gouws − *Pharmacen, Centre of Excellence for Pharmaceutical Sciences, North-West University, Potchefstroom 2520, South Africa*; Phone: +27-18-285-2505; Email: Chrisna.Gouws@nwu.ac.za

Krzysztof Wrzesinski − *Pharmacen, Centre of Excellence for Pharmaceutical Sciences, North-West University, Potchefstroom 2520, South Africa; CelVivo ApS, Blommenslyst 5491, Denmark;* orcid.org/0000-0002-0381-4523; Phone: +45-5080-9776; Email: kwr@celvivo.com

Authors

Tanya Smit − *Pharmacen, Centre of Excellence for Pharmaceutical Sciences, North-West University, Potchefstroom 2520, South Africa*

Carlemi Calitz − *Pharmacen, Centre of Excellence for Pharmaceutical Sciences, North-West University, Potchefstroom 2520, South Africa*

Clarissa Willers − *Pharmacen, Centre of Excellence for Pharmaceutical Sciences, North-West University, Potchefstroom 2520, South Africa*

Hanna Svitina − *Pharmacen, Centre of Excellence for Pharmaceutical Sciences, North-West University, Potchefstroom 2520, South Africa*

Josias Hamman − *Pharmacen, Centre of Excellence for Pharmaceutical Sciences, North-West University, Potchefstroom 2520, South Africa*

Stephen J. Fey − *CelVivo ApS, Blommenslyst 5491, Denmark;* orcid.org/0000-0001-6463-9477

Complete contact information is available at: https://pubs.acs.org/10.1021/acsmedchemlett.0c00076

Author Contributions

Conceptualization, C.G. and K.W.; methodology, K.W., C.C., T.S., and H.S.; evaluation, T.S., C.W., and H.S.; formal analysis, T.S. and H.S.; investigation, T.S., C.C., C.W., and H.S.; resources, J.H., C.G., and K.W.; data curation, T.S., H.S., C.G., and K.W.; writing-original draft preparation, T.S. and C.C.; writing-review and editing, C.C., C.W., J.H., S.J.F., C.G., and K.W.; visualization, T.S., C.C., and H.S.; supervision, J.H., C.G., and K.W.; project administration, C.G.; funding acquisition, C.G. and K.W.

Funding

This research was funded by National Research Foundation (NRF) of South Africa [Grant number 91460]; the South African Medical Research Council (MRC) [Self-Initiated Research grant] and MC2 Therapeutics (Denmark). T.S. was funded by Die Suid-Afrikaanse Akademie vir Wetenskap en Kuns. Opinions expressed, and conclusions arrived at, are those of the author and are not necessarily to be attributed to the NRF or the MRC. S.J.F., C.G., and K.W. would like to acknowledge the support of the COST actions CM1407 (Challenging organic synthesis inspired by nature—from natural products chemistry to drug discovery) and CA16119 (*In vitro* 3-D total cell guidance and fitness). The funding sponsors had no role in the design of the study; in the collection, analyses, or interpretation of data; in the writing of the manuscript, and in the decision to publish the results.

Notes

The authors declare no competing financial interest.

ABBREVIATIONS

3D, three-dimensional; 2D, two-dimensional; AK, adenylate kinase; ANOVA, one-way analysis of variance; ATP, adenosine triphosphate; BAM, BioArray Matrix drive; BSA, bovine serum albumin; cDNA, complementary DNA; DMEM, Dulbecco's modified Eagle's medium; FBS, fetal bovine serum; GAPDH, glyceraldehyde 3-phosphate dehydrogenase; IC_{50}, 50% inhibitory concentration; MTT, 3-(4,5-dimethylthiazol-2-yl)- 2,5-diphenyltetrazolium bromide assay; mRNA, mRNA; P-gp, P-glycoprotein; PXR, pregnane X receptor; qRT-PCR, real-time polymerase chain reaction; RNA, ribonucleic acid; SCLC, small cell lung cancer; TBP, TATA-box binding protein

REFERENCES

(1) Katzung, B. G.; Masters, S. B.; Trevor, A. J. *Basic and Clinical Pharmacology*, 12th ed.; McGraw-Hill: New York, 2012; pp 949−965.

(2) Mishra, J.; Drummond, J.; Quazi, S. H.; Karanki, S. S.; Shaw, J. J.; Chen, B.; Kumar, N. Prospective of colon cancer treatments and scope for combinatorial approach to enhanced cancer cell apoptosis. *Crit. Rev. Oncol. Hemat.* **2013**, *86*, 232−250.

(3) Naghibalhossaini, F.; Shefaghat, M.; Mansouri, A.; Jaberi, H.; Tatar, M.; Eftekhar, E. The impact of thymidylate synthase and methylenetetrahydrofolate reductase genotypes on sensitivity to 5-Fluorouracil treatment in colorectal cancer cells. *Acta Med. Iran.* **2017**, *55*, 751−758.

(4) Singh, S.; Sharma, B.; Kanwar, S. S.; Kumar, A. Lead phytochemicals for anticancer drug development. *Front. Plant Sci.* **2016**, *7*, 1−13.

(5) Simmonds, P. C. Palliative chemotherapy for advanced colorectal cancer: systematic review and meta-analysis. *Colorect. Cancer Collab. Group.* **2000**, *321*, 531−535.

(6) Van Cutsem, E.; Köhne, C. H.; Hitre, E.; Zaluski, J.; Chang Chien, C. R.; Makhson, A.; D'Haens, G.; Pintér, T.; Lim, R.; Bodoky, G.; Roh, J. K. Cetuximab and chemotherapy as initial treatment for metastatic colorectal cancer. *N. Engl. J. Med.* **2009**, *360*, 1408−1417.

(7) Koziara, J. M.; Whisman, T. R.; Tseng, M. T.; Mumper, R. J. *In vivo* efficacy of novel paclitaxel nanoparticles in paclitaxel-resistant human colorectal tumors. *J. Controlled Release* **2006**, *112*, 312−319.
(8) Grimm, D. 2019. U.S. EPA to eliminate all mammal testing by 2035. Available online: URL https://www.sciencemag.org/news/2019/09/us-epa-eliminate-all-mammal-testing-2035 (accessed on 2019-10-03).
(9) Jaroch, K.; Jaroch, A.; Bojkoa, B. Cell cultures in drug discovery and development: The need of reliable *in vitro-in vivo* extrapolation for pharmacodynamics and pharmacokinetics assessment. *J. Pharm. Biomed. Anal.* **2018**, *147*, 297−312.
(10) Gouws, C.; Hamman, J. H. Recent developments in our understanding of the implications of traditional African medicine on drug metabolism. *Expert Opin. Drug Metab. Toxicol.* **2018**, *14*, 161−168.
(11) Hariparsad, N.; Sane, R. S.; Strom, S. C.; Desai, P. B. *In vitro* methods in human drug biotransformation research: implications for cancer chemotherapy. *Toxicol. In Vitro* **2006**, *20*, 135−153.
(12) Xu, X.; Farach-Carson, M. C.; Jia, X. Three-dimensional *in vitro* tumor models for cancer research and drug evaluation. *Biotechnol. Adv.* **2014**, *32*, 1256−1268.
(13) Saeidnia, S.; Manayi, A.; Abdollahi, M. From *in vitro* Experiments to *in vivo* and Clinical Studies; Pros and Cons. *Curr. Drug Discovery Technol.* **2016**, *12*, 218−224.
(14) Goodspeed, A.; Heiser, L. M.; Gray, J. W.; Costello, J. C. Tumor-derived cell lines as molecular models of cancer pharmacogenomics. *Mol. Cancer Res.* **2016**, *14*, 3−13.
(15) Wong, C. H.; Siah, K. W.; Lo, A. W. Estimation of clinical trial success rates and related parameters. *Biostat.* **2019**, *20*, 273−286.
(16) Mouradov, D.; Sloggett, C.; Jorissen, R. N.; Love, C. G.; Li, S.; Burgess, A. W.; Arango, D.; Strausberg, R. L.; Buchanan, D.; Wormald, S.; O'Connor, L. Colorectal cancer cell lines are representative models of the main molecular subtypes of primary cancer. *Cancer Res.* **2014**, *74*, 3238−3247.
(17) Tsujimoto, M.; Agawa, C.; Ueda, S.; Yamane, T.; Kitayama, H.; Terao, A.; Fukuda, T.; Minegaki, T.; Nishiguchi, K. Inhibitory effects of juices prepared from individual vegetables on CYP3A4 activity in recombinant CYP3A4 and LS180 cells. *Biol. Pharm. Bull.* **2017**, *40*, 1561−1565.
(18) Engman, H. A.; Lennernäs, H.; Taipalensuu, J.; Otter, C.; Leidvik, B.; Artursson, P. CYP3A4, CYP3A5, and MDR1 in human small and large intestinal cell lines suitable for drug transport studies. *J. Pharm. Sci.* **2001**, *90*, 1736−1751.
(19) Brandon, E. F. A.; Bosch, T. M.; Deenena, M. J.; Levinka, R.; Van der Wal, E.; Van Meerveld, J. B. M.; Bijl, M.; Beijnen, J. H.; Schellens, J. H. M.; Meijerman, I. Validation of *in vitro* cell models used in drug metabolism and transport studies; genotyping of cytochrome P450, phase II enzymes and drug transporter polymorphisms in the human hepatoma (HepG2), ovarian carcinoma (IGROV-1) and colon carcinoma (CaCo-2, LS180) cell lines. *Toxicol. Appl. Pharmacol.* **2006**, *211*, 1−10.
(20) Brandin, H.; Viitanen, E.; Myrberg, O.; Arvidsson, A. K. Effects of herbal medicinal products and food supplements on induction of CYP1A2, CYP3A4 and MDR1 in the human colon carcinoma cell line LS180. *Phytother. Res.* **2007**, *21*, 239−244.
(21) Gupta, A.; Mugundu, G. M.; Desai, P. B.; Thummel, K. E.; Unadkat, J. D. Intestinal human colon adenocarcinoma cell line LS180 is an excellent model to study pregnane X receptor, but not constitutive androstane receptor, mediated CYP3A4 and multidrug resistance transporter 1 induction: Studies with anti-human immunodeficiency virus protease inhibitors. *Drug Metab. Dispos.* **2008**, *36*, 1172−1180.
(22) Antoni, D.; Burckel, H.; Josset, E.; Noel, G. Three-dimensional cell culture: A breakthrough *in vivo*. *Int. J. Mol. Sci.* **2015**, *16*, 5517−5527.
(23) Fang, Y.; Eglen, R. M. Three-dimensional cell cultures in drug discovery and development. *3D Cell Cult. Drug Screen. Optim.* **2017**, *22*, 456−472.
(24) Fey, S. J.; Wrzesinski, K. Determination of drug toxicity using 3D spheroids constructed from an immortal human hepatocyte cell line. *Toxicol. Sci.* **2012**, *127*, 403−11.
(25) Wrzesinski, K.; Fey, S. J. From 2D to 3D - a new dimension for modelling the effect of natural products on human tissue. *Curr. Pharm. Des.* **2015**, *21*, 5605−5616.
(26) Nunes, A. S.; Barros, A. S.; Costa, E. C.; Moreira, A. F.; Correia, I. J. 3D tumor spheroids as *in vitro* models to mimic *in vivo* human solid tumor resistance to therapeutic drugs. *Biotechnol. Bioeng.* **2019**, *116*, 206−226.
(27) Haycock, J. W. 3D cell culture: a review of current approaches and techniques. In *3D cell culture: methods and protocols*; Springer Science+Business Media: Switzerland, 2011; pp 1−15.
(28) McKee, C.; Chaudhry, G. R. Advances and challenges in stem cell culture. *Colloids Surf., B* **2017**, *159*, 62−77.
(29) Khetani, S. R.; Bhatia, S. N. Engineering tissues for *in vitro* applications. *Curr. Opin. Biotechnol.* **2006**, *17*, 524−531.
(30) Martin, I.; Wendt, D.; Heberer, M. The role of bioreactors in tissue engineering. *Trends Biotechnol.* **2004**, *22*, 80−86.
(31) Kapałczyńska, M.; Kolenda, T.; Przybyła, W.; Zajączkowska, M.; Teresiak, A.; Filas, V.; Ibbs, M.; Bliźniak, R.; Łuczewski, Ł.; Lamperska, K. 2D and 3D cell cultures−a comparison of different types of cancer cell cultures. *Arch. Med. Sci.* **2016**, *14*, 910.
(32) Tan, W. H.; Takeuchi, S. Monodisperse alginate hydrogel microbeads for cell encapsulation. *Adv. Mater.* **2007**, *19*, 2696−2701.
(33) Le Roux, M. A.; Guilak, F.; Setton, L. A. Compressive and shear properties of alginate gel: effects of sodium ions and alginate concentration. *J. Biomed. Mater. Res.* **1999**, *47*, 46−53.
(34) Lee, K. Y.; Mooney, D. J. Alginate: properties and biomedical applications. *Prog. Polym. Sci.* **2012**, *37*, 106−126.
(35) Gombotz, W. R.; Wee, S. Protein release from alginate matrices. *Adv. Drug Delivery Rev.* **1998**, *31*, 267−285.
(36) Chung, T. W.; Yang, J.; Akaike, T.; Cho, K. Y.; Nah, J. W.; Kim, S. I.; Cho, C. S. Preparation of alginate/galactosylated chitosan scaffold for hepatocyte attachment. *Biomaterials* **2002**, *23*, 2827−2834.
(37) Murua, A.; Portero, A.; Orive, G.; Hernández, R. M.; de Castro, M.; Pedraz, J. L. Cell microencapsulation technology: towards clinical application. *J. Controlled Release* **2008**, *132*, 76−83.
(38) Wang, L.; Shelton, R. M.; Cooper, P. R.; Lawson, M.; Triffitt, J. T.; Barralet, J. E. Evaluation of sodium alginate for bone marrow cell tissue engineering. *Biomaterials* **2003**, *24*, 3475−3481.
(39) Akcay, A. The calculation of LD50 using probit analysis. *FASEB J.* **2013**, *27*, 1217−1218.
(40) Rossouw, M. J. *Evaluation of the efficacy of selected anticancer compounds in multidrug resistant cell culture models*. Potchefstroom: NWU, 2018 (Dissertation-MSc).
(41) Bröker, L. E.; Kruyt, F. A.; Giaccone, G. Cell death independent of caspases: a review. *Clin. Cancer Res.* **2005**, *11*, 3155−3162.
(42) Ahmann, F. R.; Garewal, H. S.; Schifman, R.; Celniker, A.; Rodney, S. Intracellular adenosine triphosphate as a measure of human tumor cell viability and drug modulated growth. *In Vitro Cell. Dev. Biol.* **1987**, *23*, 474−480.
(43) Kijanska, M.; Kelm, J. 2016. *In vitro* 3D spheroids and microtissues: ATP-based cell viability and toxicity assays. In *Assay Guidance Manual*; Sittampalam, G. S., Coussens, N. P., Brimacombe, K., Grossman, A., Arkin, M., Auld, A., Austin, C., Baell, J., Bejcek, B., Chung, T. D. Y., Dahlin, J. L., Devanaryan, V., Foley, T. L., Glicksman, M., Hall, M. D., Hass, J. V., Inglese, J., Iversen, P. W., Kahl, S. D., Kales, S. C., Lal-Nag, M., Li, Z., McGee, J., McManus, O., Riss, T., Trask, O. J., Weidner, J. R., Xia, M., Xu, X., Eds.; Eli Lilly & Company and the National Center for Advancing Translational Sciences: Bethesda, pp 355−385.
(44) Leist, M.; Single, B.; Naumann, H.; Fava, E.; Simon, B.; Kühnle, S.; Nicotera, P. Inhibition of mitochondrial ATP generation by nitric oxide switches apoptosis to necrosis. *Exp. Cell Res.* **1999**, *249*, 396−403.

https://dx.doi.org/10.1021/acsmedchemlett.0c00076
ACS Med. Chem. Lett. XXXX, XXX, XXX−XXX

(45) Kanduc, D.; Mittelman, A.; Serpico, R.; Sinigaglia, E.; Sinha, A. A.; Natale, C.; Santacroce, R.; Di Corcia, M. G.; Lucchese, A.; Dini, L.; Pani, P.; Santacroce, S.; Simone, S.; Bucci, R.; Farber, E. Cell death: apoptosis versus necrosis. *Int. J. Oncol.* **2002**, *21*, 165−170.
(46) Elmore, S. Apoptosis: a review of programmed cell death. *Toxicol. Pathol.* **2007**, *35*, 495−516.
(47) Jacobs, A. C.; DiDone, L.; Jobson, J.; Sofia, M. K.; Krysan, D.; Dunman, P. M. Adenylate kinase release as a high-throughput-screening-compatible reporter of bacterial lysis for identification of antibacterial agents. *Antimicrob. Agents Chemother.* **2013**, *57*, 26−36.
(48) Leist, M.; Jäättelä, M. Four deaths and a funeral: from caspases to alternative mechanisms. *Nat. Rev. Mol. Cell Biol.* **2001**, *2*, 589−599.
(49) Squirrell, D.; Murphy, J. Rapid detection of very low numbers of micro-organisms using adenylate kinase as a cell marker. *A practical guide to industrial uses of ATP luminescence in rapid microbiology*; 1997; pp 107−113.
(50) Wrzesinski, K.; Magnone, M. C.; Hansen, L. V.; Kruse, M. E.; Bergauer, T.; Bobadilla, M.; Gubler, M.; Mizrahi, J.; Zhang, K.; Andreasen, C. M.; Joensen, K. E. HepG2/C3A 3D spheroids exhibit stable physiological functionality for at least 24 days after recovering from trypsinisation. *Toxicol. Res.* **2013**, *2*, 163−172.
(51) Wrzesinski, K.; Fey, S. Metabolic reprogramming and the recovery of physiological functionality in 3D cultures in micro-bioreactors. *Bioengineering* **2018**, *5*, 1−25.
(52) Synold, T. W.; Dussault, I.; Forman, B. M. The orphan nuclear receptor SXR coordinately regulates drug metabolism and efflux. *Nat. Med.* **2001**, *7*, 584−590.
(53) Li, Q.; Sai, Y.; Kato, Y.; Tamai, I.; Tsuji, A. Influence of drugs and nutrients on transporter gene expression levels in CaCo-2 and LS180 intestinal epithelial cell lines. *Pharm. Res.* **2003**, *20*, 1119−1124.
(54) Hoarau-Véchot, J.; Rafii, A.; Touboul, C.; Pasquier, J. Halfway between 2D and animal models: are 3D cultures the ideal tool to study cancer-microenvironment interactions? *Int. J. Mol. Sci.* **2018**, *19*, 181.
(55) Shandiz, S. A. S.; Salehzadeh, A.; Ahmadzadeh, M.; Khalatbari, K. Evaluation of cytotoxicity activity and NM23 gene expression in T47D breast cancer cell line treated with Glycyrrhiza glabra extract. *J. Genet. Resour.* **2017**, *3*, 47−53.
(56) Livak, K. J.; Schmittgen, T. D. Analysis of relative gene expression data using real-time quantitative PCR and the 2-ΔΔCT method. *Methods* **2001**, *25*, 402−408.

https://dx.doi.org/10.1021/acsmedchemlett.0c00076
ACS Med. Chem. Lett. XXXX, XXX, XXX−XXX